Spatial scales of temperature and salinity variability estimated from Argo observations

F. Ninove[1], P.Y. Le Traon[1,2], E. Remy[2] and S. Guinehut[3]

[1] {Ifremer, Plouzané, France}

[2] {Mercator Ocean, Ramonville Saint Agne, France}

Correspondence to: P.-Y. Le Traon (pierre-yves.letraon@mercator-ocean.fr)

Abstract

Argo observations from 2005 to 2013 are used to characterize spatial scales temperature and salinity variations from the surface down to 1500 m. Simulations are first performed to analyze the sensitivity of results to Argo sampling; they show that several years of Argo observations are required to estimate of spatial scales of ocean variability over 20°x20° boxes. Spatial scales are then computed over several large scale areas. Zonal and meridional spatial scales (Lx and Ly which are also zero crossing of covariance functions) vary as expected with latitudes. Scales are of about 100 km at high latitudes and more of 700 km in the Indian and Pacific equatorial/tropical regions. Zonal and meridional scales are similar except in these tropical/equatorial regions where zonal scales are much larger (by a factor of 2 to 3) than meridional scales. Spatial scales are the largest close to the surface and have a general tendency for temperature to increase in deeper layers. There are significant differences between temperature and salinity scales, in particular, in the deep ocean. Results are consistent with previous studies based on sparse in-situ observations or satellite altimetry. They provide, however, for the first time a global description of temperature and salinity scales of variability and a characterization of their variations according to depths.

1 Introduction

Thanks to outstanding international cooperation, Argo the global array of profiling floats (Roemmich et al., 2009) reached its initial target of 3000 floats in operation in 2007. Argo floats measure every 10 days temperature and salinity from the surface down to 2000 m and deliver their data both in real time for operational users and after scientific quality control for climate change research and monitoring. Argo has revolutionized oceanography by providing for the first time a near real time global description of the ocean state that is fully complementary to satellite observations. An overview of Argo achievements is given in Freeland et al. (2010). Argo data have been used to better understand

global and regional sea level rise and ocean heat content variations (e.g. von Schuckmann and Le Traon, 2011), to analyze large scale ocean circulation and mesoscale variations (e.g. Roemmich et al; 2007; Dong et al., 2014) and large scale salinity variations related to the global hydrological cycle (Durack and Wijffels, 2010). Argo has strong complementarities with satellite altimetry and Argo data are now systematically used together with altimeter data for ocean analysis and forecasting (e.g. Guinehut et al., 2012; Le Traon, 2013; Oke et al., 2015).

The availability of global temperature and salinity data sets over several years is a unique opportunity to better characterize the statistics of ocean mesoscale variability at global scale. Although Argo does not resolve mesoscale variability due to its 3°x3° spatial sampling, it is very well suited to estimate its main statistical characteristics. Guinehut et al. (2012) derived, for example, statistical relationships between surface and subsurface fields to infer the 3D mesoscale T&S fields from altimetry and sea surface temperature (SST) and Argo observations. We focus here on the spatial scales of temperature and salinity variations. Over several years and in given region, there are many nearly simultaneous pairs of floats with different separation distances allowing an estimation of such scales. These estimations are important to better characterize and understand ocean dynamics and to improve quality control, mapping or data assimilation schemes (e.g. Gaillard et al., 2009; Roemmich and Gilson, 2009). They are also essential to refine the sampling requirements for the Argo global array as an optimal sampling should reflect the actual spatial (and time) scales of ocean variability.

The paper is organized as follows. Data and methods are presented in section 2. The capability of Argo sampling to estimate spatial correlation scales is analyzed with simulated data in section 3. Section 4 provides a global calculation of spatial scales and discusses the main results. Conclusions and perspectives are given in section 5.

2 Data sets and methods

We used Argo observations from 2005 to 2013 as obtained from the Coriolis data center. Data from 2005 to 2012 are delayed mode quality controlled data from the CORA data base (Cabanes et al., 2013). Data from 2013 are near real time data from the Coriolis Argo Global Data Assembly Center (one of the two Argo GDACs). An additional quality control with regional climatology checks was applied to these near real time data sets.

After several tests (see discussion in section 3), correlation scales were calculated over several large scale areas to provide sufficient pair of observations at different zonal and meridional distances. Correlations were computed both for temperature and salinity and for the surface down to 1300 m. The following steps are used for the calculation:

1. The Levitus 2009 seasonal climatology is removed from Argo profile observations.

2. All temperature and salinity Argo data (from 2005 to 2013) within a given box (e.g. 20° latitude x20° longitude up to 20° latitude x 100° longitude) are gathered and a large scale (4°x4°) seasonal mean of observations is computed and removed from the observations. This allows removing possible biases in the climatology. Data are then stored in weekly files.

3. The covariance for a given zonal (dx) and meridional (dy) distance is then calculated as:

   $Cov(dx, dy) = Var - 0.5\ \gamma(dx, dy)$,

   $\gamma(dx, dy) = 1/N \sum_{\text{all weeks}} \sum_{ij} (z'(xi,yi,ti)-z'(xj,yj,tj))^2$,

   where var is the variance, γ is the variogram and z' is the anomaly of temperature or salinity at a given depth and N is the number of pairs of Argo profiles whose zonal (xi-xj) and meridional (yi-yj) distances are comprised between dx ± 12.5 km and dy ± 12.5 km and whose time separations are comprised between ± 3.5 days. The calculation is done with a spatial zonal and meridional resolution of 25 km. Note that covariances were derived from a variogram calculation to reduce sensitivity of results to unknown mean fields. Since we remove large scale fields (see point 2 above) prior to the calculation, this only has a small impact on the calculation.

4. Covariances are then normalized by the variance to get correlation values:

   $Cor(dx, dy) = Cov(dx, dy)/Cov(0,0)$.

5. The formal error variance on the correlation, noted Ɛ here, is then derived following the Isserlis theorem (Bendat and Piersol, 1986) and expressed as:

   $Var(Ɛ) = 1/N^2 \sum_{\text{all weeks}} \sum_{ij} Cor(dx_{ij}, dy_{ij})^2 + Cor(dx+dx_{ij}, dy+dy_{ij}).\ Cor(dx-dx_{ij}, dy-dy_{ij})$.

   dx_{ij} and dy_{ij} are the zonal and meridional distances between Argo profile i and Argo profile j. In practice this calculation is done in an iterative way after an analytical model (see below) is fitted to covariance observations. Note that if we assume that the N pairs of observations provide uncorrelated estimations of the covariance for a given dx and dy lag (which is the case if $dx_{ij} >> dx$ or $dy_{ij} >> dy$), the formal error variance on the correlation is simply equal to the following expression:

   $Var(Ɛ) = 1/N\ [1+cor(dx,dy)]$.

   It shows that RMS errors on correlations vary as $1/\sqrt{N}$ (e.g. 100 observation pairs should lead to an error of 0.1 to 0.2).

6. An analytical correlation model is then fitted to the discrete correlation estimations through a non-linear weighted least square curve fitting method based on the Levenberg-Marquardt algorithm. Formal errors (see point 5 above) are taken into account in the adjustment (weights). The correlation model follows the covariance model proposed by Arhan and Colin de Verdière (1985).

$Cor(dx, dy) = (1/1+E)\ [1 + ar + (ar)^2/6 - (ar)^3/6]\ \exp(-ar)$ if $r \neq 0$

$Cor(dx, dy) = 1$ if $r=0$, $r = [(dx/Lx)^2 + (dy/Ly)^2]^{1/2}$.

Lx and Ly are the zonal and meridional scales (zonal and meridional zero crossings of the correlation function). E is the noise variance that represents both measurement and representativity errors. a is a constant equal to 3.337 calculated so that $[1 + a + a^2/6 - a^3/6] = 0$, i.e. Cor (dx,dy)=0 when r is equal to 1. This ensures that Lx and Ly scales correspond to zero crossing correlation scales. The fitting procedure provides estimation of Lx and Ly and of their formal errors. Another calculation of error ("standard fitting errors") is also carried out by using a least square fitting with unit weights to characterize the consistency of correlation estimations with our correlation model.

3 Sensitivity of results to sampling: a simulation study

To analyze the sensitivity of results to Argo sampling, a simulation study was performed. The main objective is to test the impact of realistic Argo sampling by using actual Argo float positions in 2005 and 2013 in the North Pacific. Over a 20°x20° box, 1600 Argo profiles were available in 2005 and about 2700 for 2013. A nominal 3°x3° Argo sampling would yield about 1800 profiles per year for a 20°x20° box. 2005 is thus close to a nominal Argo sampling and 2013 corresponds to an improved Argo sampling.

We generated 52 weekly (i.e. 1 year) simulated temperature 2D fields on a 20°x20° grid that follows the Arhan and Colin de Verdière (1985) covariance model. The 2D temperature fields were then sampled at the float positions in 2005 and 2013 and an observation noise of 10% was added (E=0.1). From these simulated Argo data, we analyzed how well covariance functions can be reconstructed following the method outlined in section 2. The calculations were done both for L=100 km and L= 400 km (isotropic field with L=Lx=Ly). Figures 1a and 1b show the estimated 2D correlation fields for the L=100 km simulation for the 2005 and 2013 sampling and the associated formal error. Figures 2a and 2b show the same results but for the L=400 km simulations. Table 1 summarizes the results for correlation scale and associated error estimations.

Results show that the estimations of correlation functions are highly sensitive to the Argo sampling. Typical error for a covariance or correlation value is about 0.25-0.4 for the 2005 sampling and 0.15-0.25 for the 2013 sampling over a one year time period. Correlation scales (assuming an a priori knowledge of the covariance function shape) can be determined with an accuracy of about 20 to 30 km for 2005 and 10 to 20 km for 2013. These results are obviously dependent on the number of observation pairs available for a given spatial dx and dy lag. Correlation errors are also larger for the 400 km simulation because there are less independent observations of correlation.

These results show that one year of Argo observations over a 20°x20° box does not allow estimating precise enough correlation functions. When the sampling is improved as in 2013, results are, however, significantly improved. These results can easily be extrapolated to longer time series (and/or larger boxes) as correlation error RMS are proportional to the number of observation pairs at a given spatial lag (see equation in section 2). RMS errors for a four year time period will thus be divided by a factor of two. In that case, we expect errors on correlation of about 0.1 to 0.2 and an error on correlation scales below 10 km.

4 Results and discussion

A preliminary calculation of spatial scales (Lx and Ly which are also zero crossing of correlation functions) was carried out over several large areas (figure 3). Calculations were done both for temperature and salinity and all depths from the surface down to 1300 meters.

As an illustration, results for one box (box 3) in the North Pacific are shown on figures 4 and 5 for temperature at two different depths (200 and 1000 m). In that box, correlations are well estimated with a typical error below 0.1 due a large number of observation pairs N for a given zonal and meridional spatial lag (N comprised between 200 and 400). The estimated zonal and meridional correlation scales are 130 km and 110 km respectively. This is consistent with results derived from altimeter data analysis in mid latitude regions (e.g. Kurugano and Kamachi, 2000; Jacobs et al., 2001; Le Traon et al., 2003). Correlation scales are significantly larger at 1000 m (figure 5) and Lx and Ly are estimated to 185 km and 160 km respectively. Salinity scales (not shown) are very close to temperature ones although the estimation is slightly noisier.

Zonal and meridional spatial scales vary as expected with latitudes. Compared to mid latitude regions, scales are much larger in the tropical and equatorial regions. Figure 6 shows, for example, the correlation function for temperature at 200 m in the whole Equatorial Pacific. Zonal and meridional scales are estimated to about 900 km and 350 km. The zonal scales are smaller than those derived from TAO observations and larger than those derived from altimeter data (e.g. Kessler et al., 1996; Jacobs et al., 2001). This may be due to both the techniques used to compute scales (e.g. removing of large scale signals before computing altimeter spatial scales) and the sparse spatial sampling of TAO observations. As expected and well observed from altimetry and in-situ observations, there is a strong anisotropy with zonal scales two to three times larger than meridional scales. It is interesting to note that, compared to the Pacific ocean, smaller zonal scales are observed in the Indian (box 9 – zonal scale of 780 km at 200 m for temperature) and Atlantic (box 8 - zonal scale of 360 km at 200 m for temperature) tropical/equatorial oceans.

They are also interesting variations of scales according to depth. Figures 7, 8 and 9 shows the vertical distribution of scales both for temperature and salinity for several areas (boxes 2, 9 and 18). At the

surface or in the mixed layer, scales are much larger because they reflect large scale atmospheric forcing (heat flux, evaporation and precipitation). Note, however, that a mean seasonal cycle is removed priori the calculation. Below the mixed layer, scales are more representative of mesoscale dynamics and are consistent with scales derived from satellite altimetry. There is a general tendency (not systematic though) for an increase of temperature scales at depths larger than 800-1000 m although the correlation functions are noisier there because of lower signals. This may reflect a smaller influence of mesoscale variability at deeper depths but this should be investigated further.

There are significant differences between salinity and temperature scales (see figures 7, 8 and 9). At the surface and in the mixed layer where we observe large spatial scales, differences may reflect differences in scales between E-P (in particular precipitation) and heat flux forcing. At mid depth and depending on regions, differences may reflect the different dynamical nature of temperature and salinity signals. It is interesting to note, in particular, that the increase of scales for depths deeper than 800-1000 m for boxes 9 and 18 is not observed for salinity as it is for temperature. In many ocean regions (in particular tropics and subtropics) and for the deep ocean, temperature variations are more important than salinity in changing density. Temperature variations are thus more representative of ocean dynamics and salinity is more acting as a tracer of circulation. In 2D ocean turbulence, a tracer would exhibit smaller scales than density (or temperature) with a less steep wavenumber spectrum (e.g. Vallis, 2006). Although we tend to observe smaller salinity scales, this should be analyzed further and globally.

A similar calculation was done by Resnyanskii et al. (2010) but with a more limited Argo data set (2005-2007). Our results are in a qualitative agreement with theirs although they found larger scales. This may be due to the differences in data sets but also to differences in the way spatial scales were computed. They did not remove, in particular, biases in the Levitus climatology and did not adjust a covariance model taking into account noise level.

5 Conclusions and perspectives

This study was a first attempt to estimate spatial scales of temperature and salinity at different depths from the Argo global ocean observing system. A careful error analysis was carried out and it shows that several years of Argo observations are required for a precise enough (error on correlation below 0.1 to 0.2) estimation of correlation functions over 20°x20° boxes. Correlation functions and associated zonal and meridional spatial scales were then calculated over several large areas over the global ocean. Scales vary from 350 to 900 km in the equatorial regions down to less than 100 km at high latitudes. Zonal and meridional scales are similar except in the Pacific and Indian tropical/equatorial regions where zonal scales are much larger (by a factor of 2 to 3) than meridional scales. These results are consistent with previous studies based on sparse in-situ observations or

satellite altimetry but they allow for the first time a global characterization, an analysis of differences of scales between temperature and salinity and the variations of scales according to depths. As the Argo array develops, more precise and/or higher resolution estimations can be derived. We plan to extend soon these analyses to time and space/time correlation estimations. Similar calculations will also be applied to characterize global eddy resolving model errors, i.e. instead of analyzing Argo observations minus climatology analyzing Argo observations minus a model guess. This is essential to improve data assimilation systems.

Acknowledgments

These data were collected and made freely available by the International Argo Program and the national programs that contribute to it. (http://www.argo.ucsd.edu, http://argo.jcommops.org). The Argo Program is part of the Global Ocean Observing System.

References

Arhan, M. and Colin De Verdière, A.: Dynamics of Eddy Motions in the Eastern North Atlantic. J. Phys. Oceanogr., 15, 153–170, 1985.

Bendat, and Piersol, A.G.: Random data analysis and measurement procedures. J.J. Wiley-Interscience Publication John Wiley and Sons, New York 1986, 566 pp., 1986.

Cabanes, C., Grouazel, A., Von Schuckmann, K., Hammon, M., Turpin, V., Coatanoan, C., Paris, F., Guinehut, S., Boone, C., Ferry, N., de Boyer Montégut, C., Carval, T., Reverdin, G., Pouliquen, S., and Le Traon, P.Y.: The CORA dataset : validation and diagnostics of in-situ ocean temperature and salinity measurements. Ocean Science, 9, 1-18, doi: 10.5194/os-9-1-2013, 2013.

Dong, C., McWilliams, J.C., Liu, Y., and Chen, D.: Global heat and salt transports by eddy movement, Nat Commun, 5, http://dx.doi.org/10.1038/ncomms4294, 2014.

Durack, P.J., and Wijffels, S.E.: Fifty-year trends in global ocean salinities and their relationship to broad-scale warming. J. Climate, 23, 4342–4362, 2010.

Freeland, H. J., Roemmich D., Garzoli, S.L, Le Traon, P.-Y., Ravichandran, M., Riser, S., Thierry, V., Wijffels, S., Belbeoch, M., Gould, J. , Grant, .F, Ignazewski, .M, King, B., Klein, B., Mork, K.A., Owens, B., Pouliquen, S., Sterl, A., Suga, .T, Suk, M.-S., Sutton, P., Troisi, A., Velez-Belchi, P. J. and Xu, J.: Argo - A Decade of Progress. Proceedings of OceanObs'09: Sustained Ocean Observations and Information for Society (Vol. 2), Venice, Italy, 21-25 September 2009, Hall, J., Harrison D.E. & Stammer, D., Eds., ESA Publication WPP-306.

Gaillard F., E. Autret, V. Thierry, P. Galaup, C. Coatanoan, and T. Loubrieu, 2009. Quality Control of Large Argo Datasets. J. Atmos. Oceanic Technol., 26, 337–351. doi: http://dx.doi.org/10.1175/2008JTECHO552.1, 2010.

Guinehut, S., Dhomps, A.-L., Larnicol, G., and P.Y. Le Traon: High resolution 3-D temperature and salinity fields derived from in situ and satellite observations, Ocean Sci., 8, 845-857, doi:10.5194/os-8-845-2012, 2012.

Jacobs, G. A., Barron, C. N., and Rhodes, R. C.: Mesoscale characteristics, J. Geophys. Res., 106, 19,581–19,595, doi:10.1029/2000JC000669, 2001.

Kessler, W.S., Spillane, M. C., McPhaden, M. J., and Harrison, D. E: Scales of Variability in the Equatorial Pacific Inferred form Tropical Atmosphere-Ocean Buoy Array. J. Climate, 9, 2999–3024. doi: http://dx.doi.org/10.1175/1520-0442, 1996.

Kuragano, T., and Kamachi, M.: Global statistical space-time scales of oceanic variability estimated from the TOPEX/POSEIDON altimeter data, J. Geophys. Res., 105, 955–974, doi:10.1029/1999JC900247, 2000.

Le Traon, P.Y., Faugère, Y., Hernandez, F., Dorandeu, J, Mertz, F, and Ablain, M.: Can we merge GEOSAT Follow-On with TOPEX/Poseidon and ERS-2 for an improved description of the ocean circulation? Journal Of Atmospheric And Oceanic Technology, 20(6), 889-895. http://dx.doi.org/10.1175/1520-0426, 2003.

Le Traon, P.Y.: From satellite altimetry to Argo and operational oceanography: three revolutions in oceanography. Ocean Science, 9(5), 901-915. Publisher's official version: http://dx.doi.org/10.5194/os-9-901-2013, 2013.

Oke, P. R., Balmaseda, M. A., Benkiran, M., Cummings, J. A., Fujii, Y., Guinehut, S., Larnicol, G., Le Traon, P.-Y., Martin, M. J., and Dombrowsky, E.: Observing System Evaluations using GODAE systems. Oceanography, 22(3), 144-153, 2009.

Resnyanskii Y.D., M.D. Tsyrulnikov, B.S. Strukov, and A.A. Zelenko: Statistical structure of spatial variability of the ocean thermohaline fields from Argo profiling data, 2005-2007. Oceanology, Vol. 50, No. 2, 149-165. DOI: 10.1134/S0001437010020013, 2010.

Roemmich, D., Gilson, J., Davis, R., Sutton, P., Wijffels, S., and Riser, S.: Decadal Spinup of the South Pacific Subtropical Gyre. J. Phys. Oceanogr., 37, 162–173. doi: http://dx.doi.org/10.1175/JPO3004.1, 2007.

Roemmich, D. and Gilson, J.: The 2004–2008 mean and annual cycle of temperature, salinity, and steric height in the global ocean from the Argo Program, Progress in Oceanography, Volume 82, Issue 2,Pages 81-100, ISSN 0079-6611, http://dx.doi.org/10.1016/j.pocean.2009.03.004, 2009.

Roemmich, D., and the Argo Steering Team: Argo: the challenge of continuing 10 years of progress. Oceanography, 22(3), 46-55, doi:10.5670/oceanog.2009.65., 2009.

Vallis, G. K.: Atmospheric and Oceanic Fluid Dynamics. Cambridge University Press, 745 pp., 2006.

von Schuckmann, K. and Le Traon, P. Y.: How well can we derive Global Ocean Indicators from Argo data ? Ocean Science, 7(6), 783-791. Publisher's official version: http://dx.doi.org/10.5194/os-7-783-2011, 2011.

Table 1: Simulation of the impact of Argo sampling on the estimation of correlation functions.

Simulation type	Estimated L	Associated error (1 σ)
L=100 km – 2005 sampling	70 km	20 km
L=100 km – 2013 sampling	89 km	11 km
L=400 km – 2005 sampling	372 km	30 km
L=400 km – 2013 sampling	418 km	20 km

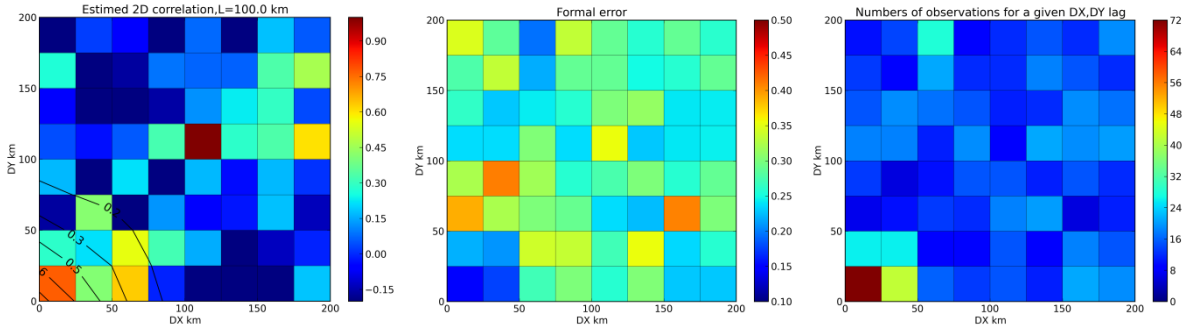

Figure 1a: Estimated 2D covariance fields for the L=100 km simulation for the 2005 Argo sampling (left), associated formal errors (middle) and number of observation pairs (right).

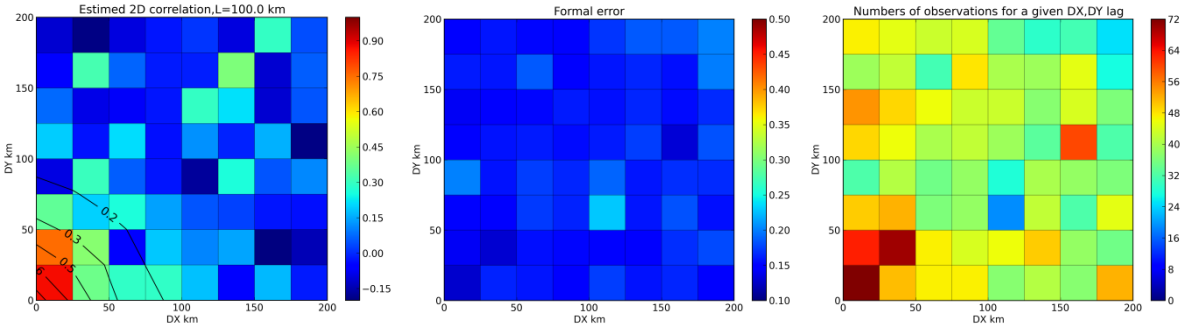

Figure 1b: Estimated 2D covariance fields for the L=100 km simulation for the 2013 Argo sampling (left), associated formal errors (middle) and number of observation pairs (right).

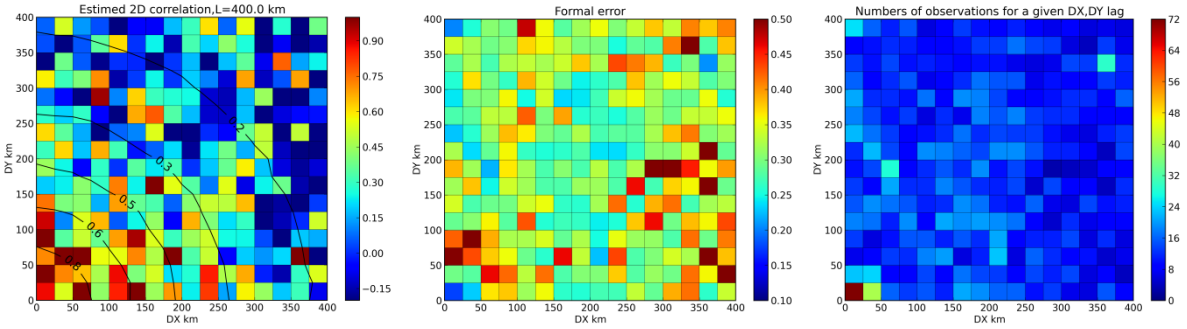

Figure 2a: Estimated 2D covariance fields for the L=400 km simulation for the 2005 Argo sampling (left), associated formal errors (middle) and number of observation pairs (right).

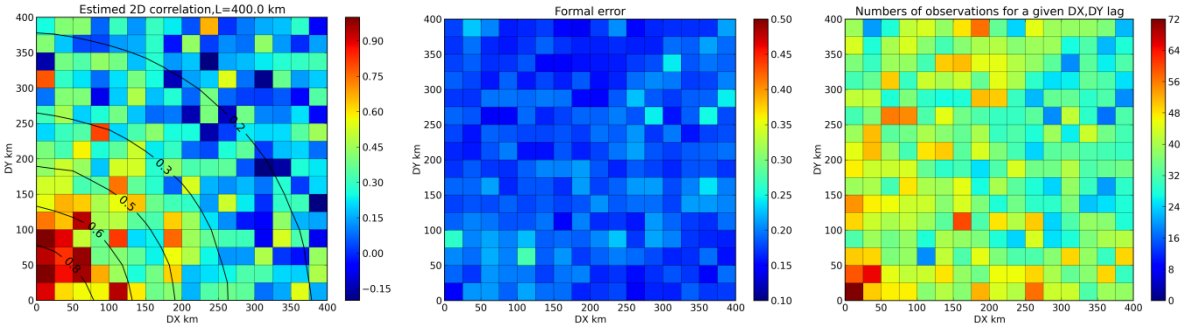

Figure 2b: Estimated 2D covariance fields for the L=400 km simulation for the 2013 Argo sampling (left), associated formal errors (middle) and number of observation pairs (right). Black isolines (left) correspond to the adjusted covariance model.

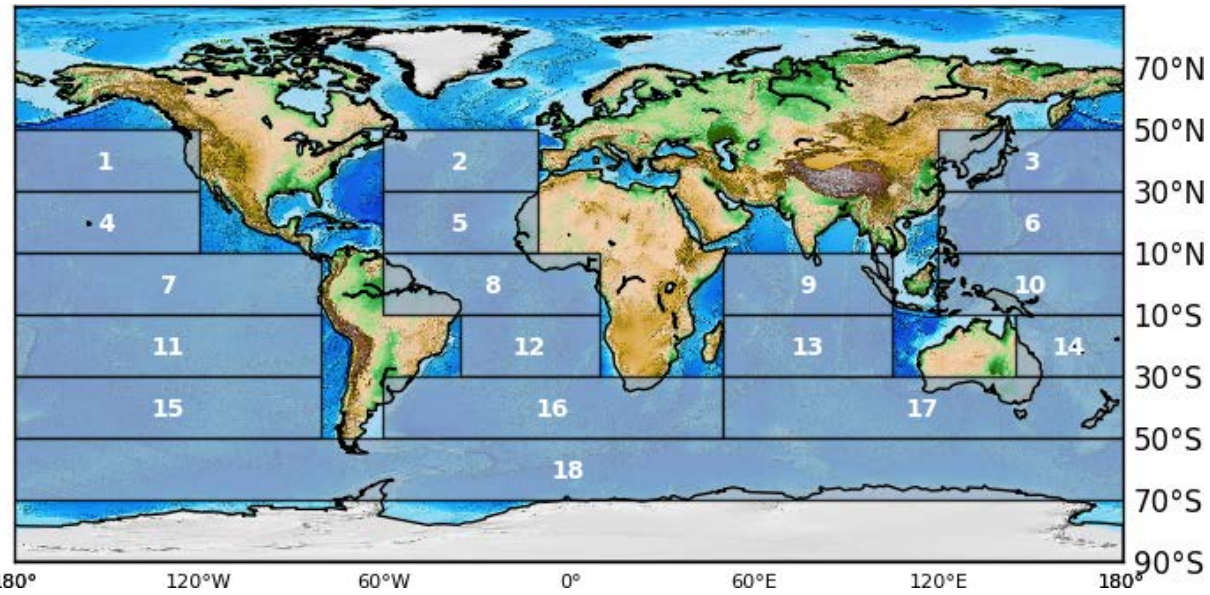

Figure 3: Large scale areas where temperature and salinity spatial correlations were calculated.

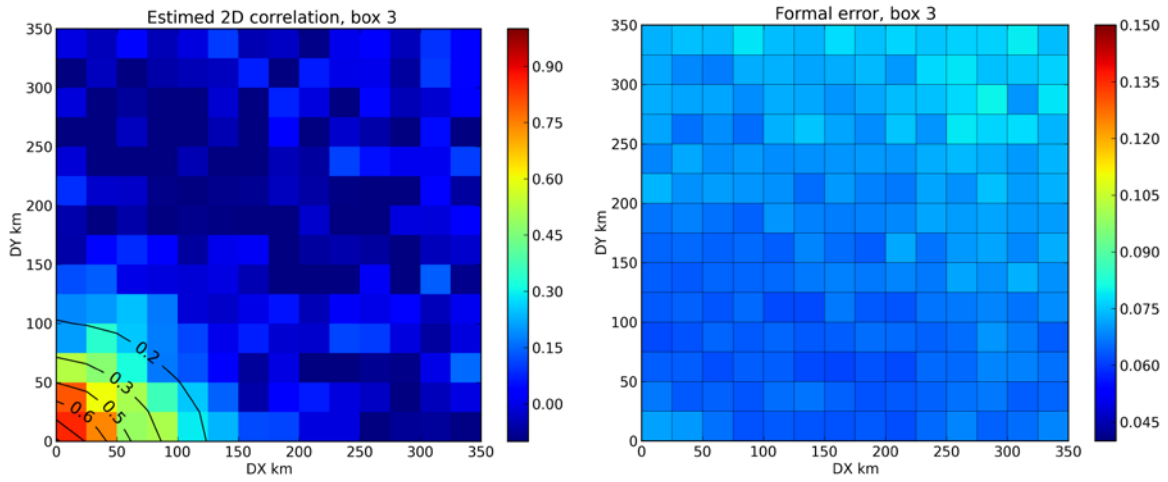

Figure 4: 2D covariance calculated in a 20°x60° area (box number 3) in the North Pacific Ocean (left) and associated formal error (right) for temperature at 200 m. Black isolines (left) correspond to the adjusted covariance model.

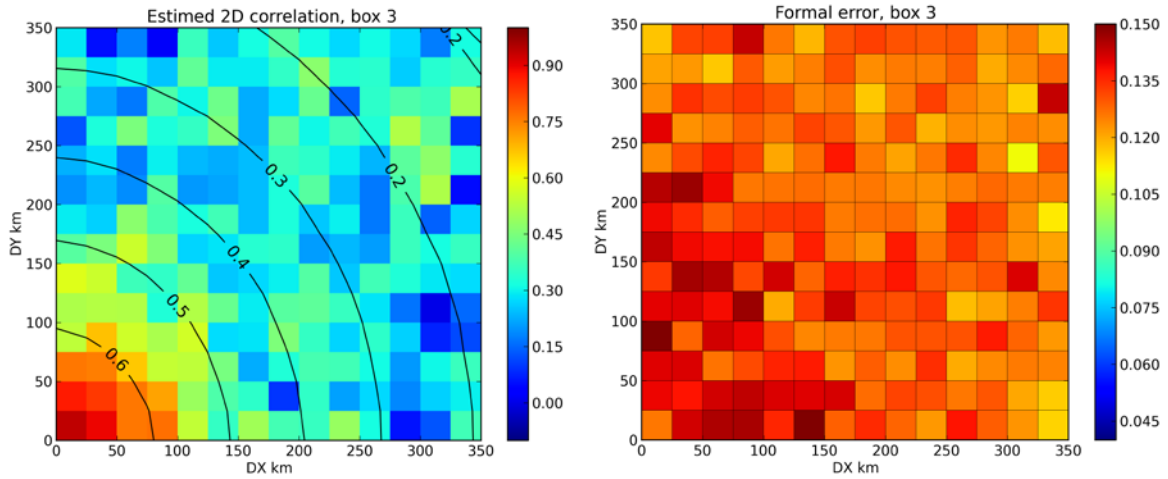

Figure 5: 2D covariance calculated in a 20°x60° area (box number 3) in the North Pacific Ocean (left) and associated formal error (right) for temperature at 1000 m. Black isolines (left) correspond to the adjusted covariance model.

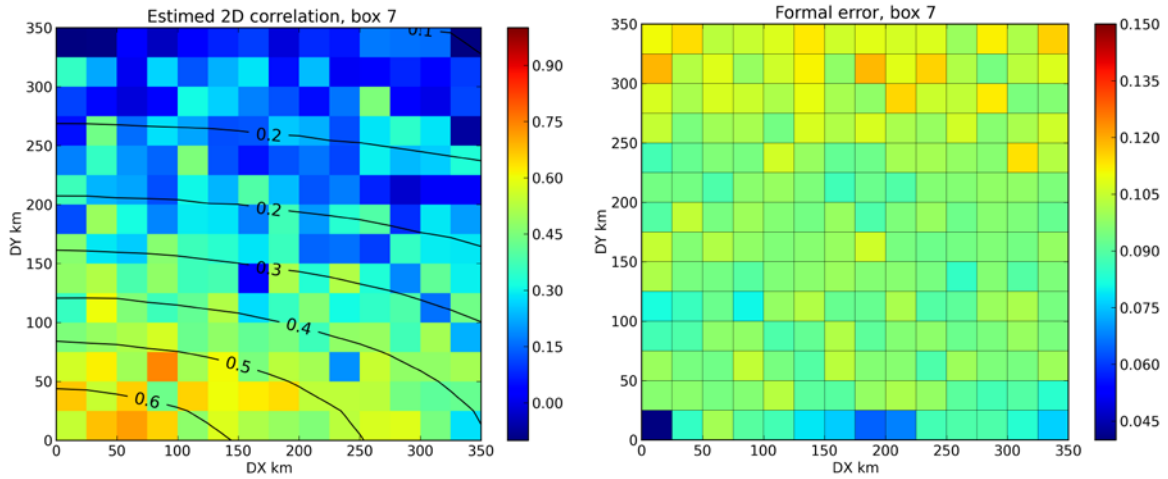

Figure 6: 2D covariance calculated in a 100°x20° area (box number 7) in the Equatorial Pacific Ocean (left) and associated formal error (right) for temperature at 200 m. Black isolines correspond to the adjusted covariance model.

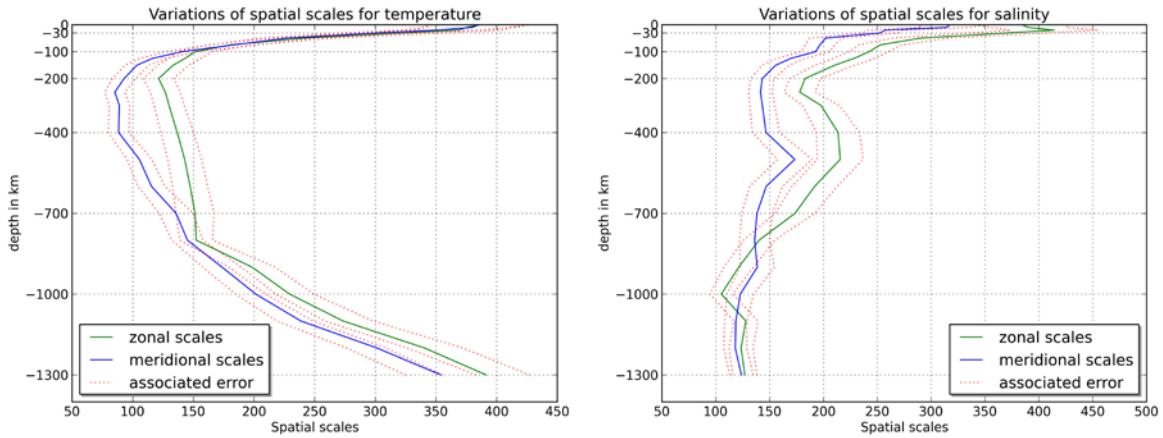

Figure 7: Variations of zonal and meridional spatial scales for temperature (left) and salinity (right) according to depth for box 18 (High latitude Southern Hemisphere). Dotted lines represent standard fitting errors.

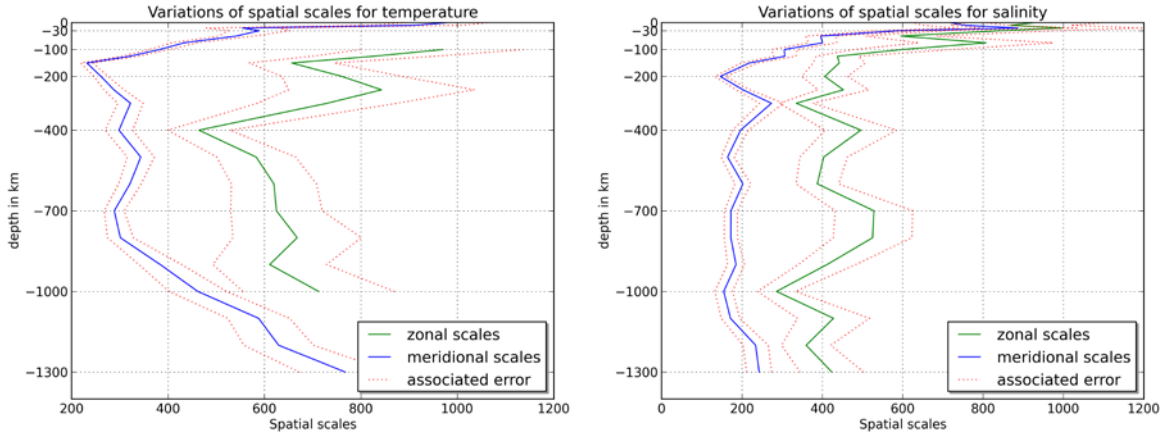

Figure 8: Variations of zonal and meridional spatial scales for temperature (left) and salinity (right) according to depth for box 9 (Equatorial Indian Pacific). Dotted lines represent standard fitting errors.

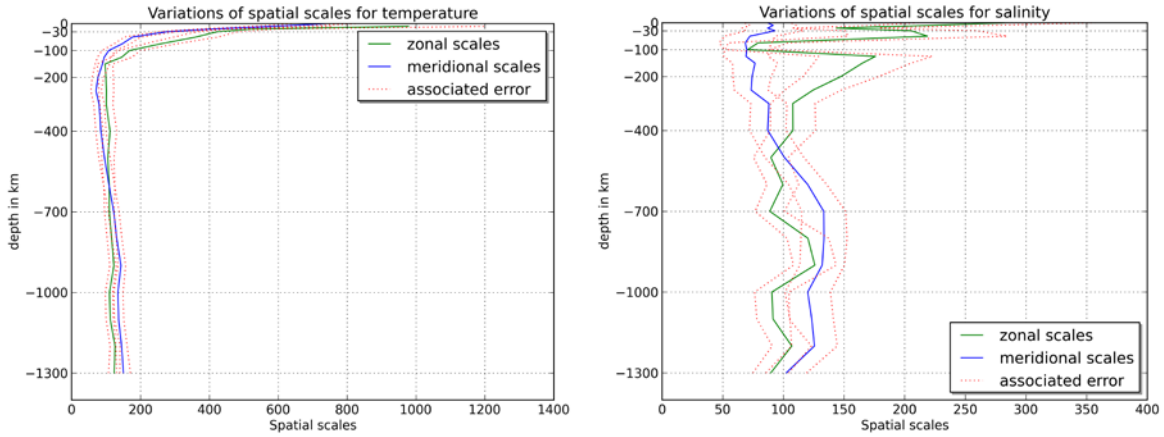

Figure 9: Variations of zonal and meridional spatial scales for temperature (left) and salinity (right) according to depth for box 2 (mid latitude North Atlantic). Dotted lines represent standard fitting errors.